GLOBAL GEOCHEMICAL VARIATION ON THE LUNAR SURFACE: A THREE-ELEMENT APPROACH. D. R.

Thomsen[1*], D. J. Lawrence[1], D. Vaniman[1], W. C. Feldman[1], R. C. Elphic[1], B. L. Barraclough[1], S. Maurice[2], P. G. Lucey[3], and A. B. Binder[4], [1]Los Alamos National Laboratory, MS D-466 Los Alamos NM, 87545, USA (* thomsend@lanl.gov), [2] S. Maurice, Observatoire Midi-Pyrenees, 14 ave Ed Belin, 31400 Toulouse, France. [3] Hawai'i Institute of Geophysics and Planetology, University of Hawai'i, Manoa HI, USA, [4] Lunar Research Institute, 1180 Sunrise Drive, Gilroy CA, 95020, USA

Introduction: We present a method for displaying the relative abundances of three important elements (thorium, iron, and titanium) on the same map projection of the lunar surface. Using Th, Fe, and Ti elemental abundances from orbital geochemical data and assigning each element a primary color, a false color map of the lunar surface was created (Fig. 1). This approach is similar to the ternary diagram approach presented by *Davis and Spudis* [1] with some important differences, discussed later. For the present maps, thorium abundances were measured by the Lunar Prospector (LP) Gamma Ray Spectrometer (GRS) [2]. The new LP GRS low altitude data set was used in this analysis [13]. Fe and Ti weight percentages were based on Clementine spectral reflectance data [3] smoothed to the LP low altitude footprint. This method of presentation was designed to aid in the location and recognition of three principal lunar compositions: ferroan anorthosite (FAN), mare basalts (MB), and the Mg suite / KREEP rich rocks on the lunar surface, with special emphasis on the highlands and specific impact basins [1], [4], [5], [6], [7], [8], [9], [10], [11], [12]. In addition to the recognition of these end-member rock compositions, this method is an attempt to examine the relationship between elemental compositions that do not conform readily to previously accepted or observed end-member rocks in various specific regions of interest, including eastern highlands regions centered on 150° longitude, and a northern highlands Th-rich region observed by *Lawrence et al.* [13].

Method: The LP low-altitude data has full-width at half-maximum spatial resolution of about 40 km [13]. The Clementine spectral reflectance data sets were adapted using an equal-area, gaussian smoothing routine to this footprint. In addition, these data sets, reported in weight percent of FeO and of TiO_2, were adjusted to Fe and Ti weight percentages. Each data set was then assigned one of the three primary colors: blue for Th, red for Fe, and green for Ti. For each element, the data range was normalized to represent the ratio of each point to the maximum in the data set. This color table provides a scheme as follows: pure red, green, or blue indicates the presence of the pure form of the respective element; white indicates the maximum values of all three elements (Th ≈ 10.3 µg/g, Fe ≈ 15.6%, and Ti ≈ 7.5%); black indicates the lack or exceedingly low values of each of the three elements. Any other color indicates a different mixture of the three. The full range of lunar longitudes is represented, but due to the lack of coverage of the Clementine data for latitudes > 70° and <-70°, the data for these regions is excluded. The differences between this approach and the ternary diagram approach of *Davis and Spudis* [1] eliminate some of the uncertainty and ambiguity of the ternary diagram approach. Rather than using a ratio of Th to Ti normalized to CI chondritic ratios, and a ternary diagram with ternary apexes located at specific end-member compositional values, elemental compositions were used independently, eliminating the errors resulting from dividing numbers that can have

high uncertainties, especially at low concentration [13].

The three elements used in this method of presentation were chosen for several reasons. One reason for the inclusion of Th in this study is that it is an accurate indicator of KREEP. Fe and Ti concentrations are both low in highland regolith, causing any small fluctuations in Th to stand out very well. In addition, Fe and Ti are good compositional indicators of different mare basalts. Mixed with red for Fe, the green for Ti produces a yellow signal in high-Ti basalts. While universally high in Fe relative to the surrounding highlands, mare basalts have a diverse range of Ti values, making Ti concentration a valuable asset to the classification and identification of different basalt types. Finally, an important constraint in element selection is the availability of the global data, both from LP and Clementine results. Data for Th, Fe, and Ti are among the highest quality of existing lunar remote sensing data. In addition, LP data for Fe and Ti will become available, enabling these data to be incorporated into the analysis.

Results: Using upper-limit values for end-member rock compositions calculated from *Korotev et al* [14], attempts were made to locate the different end-member composition of terranes on this diagram. Most strikingly, ferroan anorthosite (Th ≤ 0.37µg/g; Fe (wt%) ≤ 2.29; Ti (wt%) ≤ 0.22) [13], which should appear as an almost black, reddish color, does not appear on the diagram at any noticeable frequency. Based on this analysis, the suggestion of extensive FAN regions on the lunar surface is not strong, especially at the presently accepted values for Fe and Th. However, to make sure this effect is not due to systematic errors, a thorough investigation of the precision, accuracy, and uncertainties of the Fe, Ti, and Th abundances needs to be carried out, especially at low concentrations.

A particular region of interest is an area of high Th concentrations relative to Fe and Ti content north and east of Humboldtianum crater. First observed by *Lawrence et al* [13], this region does not coincide with any visible impact structure and comprises one of the closest approximations to pure blue (high Th, very low Ti and Fe) on the lunar surface. Such an elemental composition does not lend itself readily to classification, and presents something of an anomaly. More detailed analysis of this region is needed to understand its structure and origin.

There seems to be a longitudinal asymmetry in the Th concentrations of the highlands regolith. High Th, low Ti and Fe regions are located between 135° and 180° longitude and between -30° and +30° latitudes. While the Th levels are not high enough to attract attention in a single-elemental display, the variation in the abundance of Th relative to Fe and Ti abundances can be clearly seen. The composition that these data suggest is not well represented in the sample return suite. In addition, these regions were largely missed by the Apollo orbital ground tracks, which only covered the outer edge of the areas of interest [15]. The LP orbital Th data is the first information about the Th concentrations in

these regions of the highlands.

Regions containing MB and Mg suite / KREEP-rich compositions are readily apparent. MB deposits (average composition: Th ≈ 0.913μg/g, Fe ≈ 14.4%, and Ti ≈ 2.5%) appear as a yellowish color and appear in the Serenitatis-Tranquilitatis region, among others. This particular rock type is the most varied in color because of widespread variation in Ti content, and the contamination of these provinces by KREEP-rich material. Mafic, KREEP-rich impact melt breccias (average composition of Th ranging from 5 μg/g to concentrations higher than 10 μg/g , Fe ≈ 7.18%, and Ti ≈ 0.83%) are shown on the map as pink regions such as the ones near Copernicus and in the Jura mountains. This three-element mapping technique is advantageous in the visualization of different KREEP-rich terranes because, in contrast to the single-element Th map, this technique allows Fe and Ti compositional variations within KREEP-rich regions to be readily seen, aiding in the identification of underlying rock types, and allowing for better understanding of the processes behind KREEP emplacement.

References: [1] Davis, P. and Spudis, P. (1987) PLPSC XVII, E387-E395. [2] Lawrence, D. J. et al. (1998) *Science* **281**, 1484-1489. [3] Lucey, P. G. et al. (1999) GRL submitted. [4] Duncan A.R. et al. (1976) PLSC VII, 1659-1671. [5]McKay, G. A. et al. (1978) PLSC IX, 661-678. [6]Longhi, J. and Boudreau, A. E. (1979) PLPSC X, 2085-2105. [7] Norman, M. D. and Ryder, G. (1978) *Catalogs of Pristine Non-mare Rocks*, NASA JSC-14565 and –14603. [8]Ryder, G. (1979) PLPSC X, 561-581. [9] Norman, M. D. and Ryder, G. (1980) PLPSC X, 317-331. [10] Walker, D. (1983) PLPSC XIV in *JGR* 88, B17-B25. [11] Davis, P. and Spudis P. (1985) PLPSC XVI, D61-D74. [12] Davis P. and Spudis, P. (1986) PLPSC XVII, E84-E90. [13] Lawrence, D. J. et al. (1999) GRL submitted. [14] Korotev, R et al. (1998) JGR 103 no. E1, 1691-1701. [15] Arnold, J. et al (1977) PLSC VIII, 945.
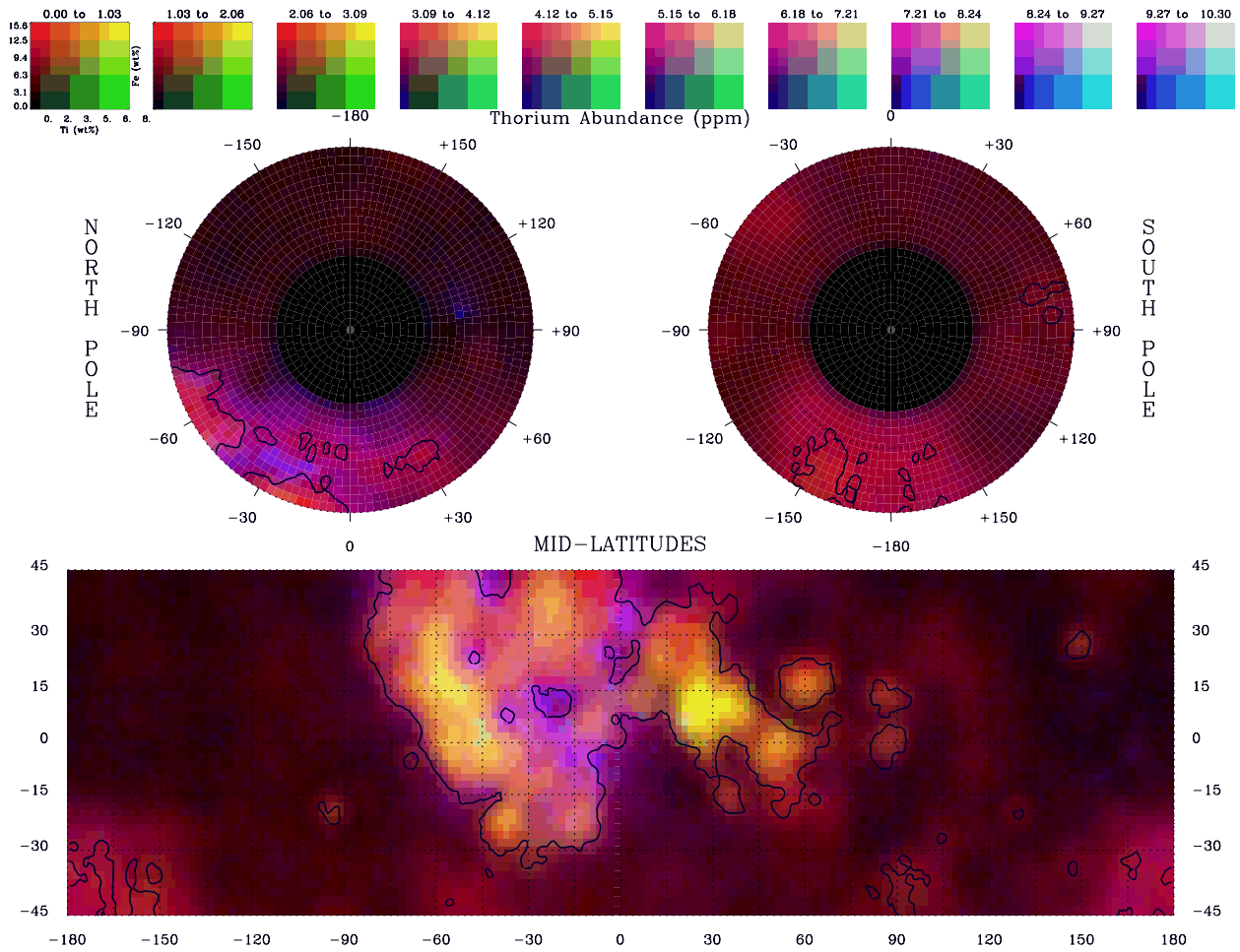

Figure 1